

Light Harvesting and Photoprotective Functions of Carotenoids in Compact Artificial Photosynthetic Antenna Designs

Gerdenis Kodis,^{*,†,‡} Christian Herrero,[†] Rodrigo Palacios,[†] Ernesto Mariño-Ochoa,[†] Stephanie Gould,[†] Linda de la Garza,[†] Rienk van Grondelle,[§] Devens Gust,[†] Thomas A. Moore,[†] Ana L. Moore,[†] and John T. M. Kennis^{*,§}

Department of Chemistry and Biochemistry and the Center for the Study of Early Events in Photosynthesis, Arizona State University, Tempe, Arizona, Department of Biophysics, Division of Physics and Astronomy, Faculty of Sciences, Vrije Universiteit, 1081 HV Amsterdam, The Netherlands, and Institute of Physics, Savanoriu 231, LT-2053 Vilnius, Lithuania

Received: July 22, 2003; In Final Form: October 10, 2003

Artificial light-harvesting constructs were synthesized by covalently linking two carotenoids to the central silicon atom of a phthalocyanine (Pc) derivative. Triad **1** binds two carotenoids having nine conjugated double bonds, whereas triad **2** binds two carotenoids having 10 carbon–carbon double bonds in conjugation. Fluorescence excitation experiments indicated that, in triad **1** dissolved in *n*-hexane, the carotenoid to Pc singlet energy transfer efficiency is ca. 92%, whereas in triad **2**, it is 30%. Results from ultrafast laser spectroscopy indicate that upon population of the optically allowed S₂ state of the carotenoid the optically forbidden states S₁ and S* are rapidly generated in both triad **1** and triad **2**. In triad **1**, S₂, S₁, and S* all contribute singlet electronic energy to Pc. In triad **2**, singlet electronic energy transfer to Pc occurs primarily from the optically allowed S₂ state with little energy transfer to Pc via the S₁ state, and there is no evidence for energy transfer via S*. Instead, in triad **2**, we find a multiphased quenching of the Pc singlet excited state on the picosecond and nanosecond time scales. Upon intersystem crossing from the singlet excited state of Pc to the triplet state in triad **1**, triplet–triplet energy transfer to either of the carotenoids takes place on a time scale significantly shorter than 5 ns. When dissolved in polar solvents, triads **1** and **2** exhibit light-induced electron transfer from either of the carotenoid moieties to the excited singlet Pc species with a time constant of about 2 ps. Charge recombination to the singlet ground state occurs in 10 ps in triad **1** and 17 ps in triad **2**.

1. Introduction

Carotenoids are indispensable in photosynthetic energy conversion, where they function as light harvesters and photoprotectors.^{1–3} They exert their light harvesting (LH) function by absorbing sunlight in the blue and green parts of the solar spectrum and transferring the energy to nearby (bacterio)chlorophyll (B)(Chl) molecules. In subsequent steps, the excitation energy is transported to the reaction center, where photochemical conversion takes place.⁴ The energy of the photons made available this way accounts for a significant fraction of photosynthetic biomass production on earth. In addition to their light-harvesting function, carotenoids assume a number of photoprotective roles. Essentially all antenna and reaction center complexes bind carotenoids to protect the organism from oxidative damage, primarily by quenching harmful (B)Chl triplet and singlet oxygen species. Recently, it has been discovered that carotenoids can act as electron donors to reduce long-lived P680⁺, and in such a way prevent damage to reactions centers of oxygenic photosynthetic organisms.^{5,6} Moreover, carotenoids appear to play a large and thus far poorly understood role in the direct quenching of Chl singlet states in

the xanthophyll cycle in Photosystem II of plants.⁷ To perform this variety of functions, carotenoids are incorporated in photosynthetic pigment–protein complexes in close contact with (B)Chl.^{8–11}

The main feature in the molecular structure of carotenoids is a polyene chain of alternating carbon–carbon single and double bonds. Until recently, the electronic states involved in the LH function have been described by one high-lying optically allowed singlet excited state (S₂) and a low-lying, optically forbidden singlet excited state (S₁). Upon light absorption, the S₂ state relaxes to the optically forbidden S₁ state in 100–200 fs by internal conversion (IC), after which the S₁ state internally converts to the ground state on the picosecond time scale.^{1,2} Recent work has shown that excited-state energy transfer (EET) from both the S₂ and S₁ states is required for efficient LH function.^{12–15} The carotenoid to (B)Chl EET processes are thought to be governed by the Coulombic coupling and the spectral overlap between donor and acceptor states,^{1,16,17} and the overall efficiency can vary from as low as 35%, for instance in the LH1 complex of *Rhodospirillum (Rs.) rubrum*¹⁸ and the PSII core complex of oxygenic photosynthesis¹⁹ to as much as 80% or more in the LHCII of plants,^{14,20} the PSI complex of cyanobacteria^{21,22} and various LH2 antennas of purple bacteria.^{1,13,15,23}

In recent years, it has become increasingly clear that the traditional description of the excited-state manifold of caro-

* To whom correspondence should be addressed. E-mail: gerdenis@asu.edu (G.K.); john@nat.vu.nl (J.T.M.K.).

[†] Arizona State University.

[‡] Institute of Physics.

[§] Vrije Universiteit.

tenoids in terms of the S_2 and S_1 states mentioned above is incomplete, and that additional optically dark states need to be considered. Koyama and co-workers presented experimental evidence concerning the existence of the theoretically predicted $^1B_u^-$ state in carotenoids by carrying out Raman excitation profile measurements.^{24,25} Subsequent ultrafast studies were interpreted in terms of an internal conversion cascade from S_2 , via $^1B_u^-$ to S_1 on the sub-100 fs time scale.^{26,27} Using multicolor femtosecond spectroscopy, we (R.v.G. and J. K.) uncovered another new optically forbidden electronic state in carotenoids, which we labeled S^* . Surprisingly, in carotenoids bound to the LH complexes of purple photosynthetic bacteria, this new S^* state is the precursor on an ultrafast reaction pathway to the carotenoid triplet state.¹⁸ To explain the ultrafast triplet formation, a singlet fission mechanism was invoked by which the S^* singlet state separates into a pair of triplet states localized on separate parts of the polyene chain, thereby conserving a total singlet spin. In subsequent work, we obtained clear evidence that S^* is active as an excited-state energy donor to BChl in bacterial LH complexes.²³ So far, the only information we have on the new S^* state is phenomenological: we know its optical absorption properties and its dynamical behavior. Its nature, identity, and origin have remained elusive. Given its ability to generate triplets, we suggested that S^* may correspond to one of the "covalent" optically dark states, like the $^1B_u^-$ state, which exhibits a doubly excited triplet character.²⁸

The development and study of simple artificial photosynthetic antennas serve a number of goals. On one hand, technological development of organic photovoltaic devices could greatly benefit from insights and design considerations that derive from artificial systems. As carotenoids constitute an integral part of the natural photosynthetic machinery where they have a multitude of functions, it would appear advantageous to incorporate them into artificial antennas. On the other hand, artificial light-harvesting antennas can be designed in a minimalist way to exert specific functions, like maximizing absorption cross sections, accessing certain spectral windows, and carrying out efficient energy transport or photoprotection in its various forms. The basic simplicity of artificial antenna systems has important advantages over the invariably far more complex natural photosynthetic systems. Their specific photo-physics can be related to unambiguous energetic, electronic, and structural features through the use of advanced spectroscopic methods, and this may yield important insights into many aspects of natural photosynthesis.^{29–32}

In this report, we have investigated the light-harvesting and photoprotective function of carotenoids in simple artificial photosynthetic antennas that consist of a phthalocyanine (Pc) moiety, to which a pair of carotenoids have been covalently linked in an axial way (Figure 1). By varying the number of carbon–carbon conjugated double bonds of the carotenoid moieties in the triads, we have studied the influence of the relative energy levels of carotenoid and Pc on their designed functions. Spectroscopic studies show that these simple antennas are capable of performing light harvesting, photoprotective, and electron transfer processes, and the mechanisms, pathways, and electronic states involved are highly reminiscent of those in natural photosynthesis.

2. Materials and Methods

Synthesis. *Dicarotenophthalocyanine 1 (Triad 1).* Methyl 8'-apo- β -caroten-8'-oate (**3**) was prepared by published procedures,³³ and 8'-apo- β -caroten-8'-oic acid was prepared by base-catalyzed hydrolysis of **3**. The coupling reaction between 8'-

apo- β -caroten-8'-oic acid and silicon tetra-*tert*-butylphthalocyanine dihydroxide (**2**, Aldrich, mixture of regioisomers) to generate triad **1** has been described.²⁹ ^1H NMR (500 MHz, CDCl_3) δ -0.21 (6H, s, car H-19'), 1.02 (12H, s, car H-16, H-17), 1.41 (6H, s, car H-20'), 1.45–1.47 (4H, m, car H-2), 1.60–1.62 (4H, m, car H-3), 1.71 (6H, s, car H-18), 1.81–1.83 (36H, m, Pc H-1'), 1.98 (6H, s, car H-19), 1.99 (6H, s, car H-20), 2.01 (4H, t, J = 6.0, car H-4), 3.59 (2H, d, J = 11.5, car H-10'), 5.08 (2H, d, J = 14.5, car H-12'), 5.19 (2H, d, d, J = 13.0, 11.5), 5.81 (2H, d, J = 12.0, car H-14'), 6.11 (2H, d, J = 7.0, car H-14), 6.13–6.17 (6H, m, car H-7, H-8, H-10), 6.30 (2H, d, J = 15.5, car H-12), 6.35 (2H, d, d, J = 13.5, 13.5, car H-15'), 6.58 (2H, d, d, J = 13.0, 13.0, car H-15) 6.67 (2H, d, d, J = 13.5, 12.0, car H-11), 8.44 (4H, d, J = 8.0, Pc H-2(3), H-9(10), H-16(17), H-23(24)), 9.58–9.74 (8H, m, Pc H-1, H-4, H-11, H-15, H-18, H-22, H-25); (MALDI-TOF) m/z 1628 (M)⁺, calc. for $\text{C}_{108}\text{H}_{126}\text{N}_8\text{O}_4$ 1628.3; UV/VIS (Toluene) 693(Pc), 662-(Pc), 622(Pc), 478(C), 452 (C) and 366(Pc) nm.

Dicarotenophthalocyanine 2 (Triad 2). Methyl 6'-apo- β -caroten-6'-oate (**4'**) was synthesized according to previous methods (same as above). The corresponding acid, 6'-apo- β -caroten-6'-oic acid, was obtained by basic hydrolysis. This acid (94.8 mg, 0.21 mmol) was transformed to the corresponding acid chloride by dissolving it in 5 mL of a 4:1 toluene:pyridine solution and adding 6 drops of thionyl chloride. The reaction mixture was stirred under a nitrogen atmosphere for 10 min, and then the solvents were removed under high vacuum. A solution of silicon tetra-*tert*-butyl-phthalocyanine dihydroxide (**2**, Aldrich, mixture of regioisomers) (20.4 mg, 0.025 mmol) in 2-picoline (4 mL, distilled from CaH_2) was added to the carotenoid acid chloride. Stirring continued under a nitrogen atmosphere for 4 h at 60 °C. At this time, 30 mg of 4-(dimethylamino)pyridine (DMAP) was added, and the mixture was allowed to react for another 24 h. Purification was done by column chromatography (silica, 6:4 CH_2Cl_2 :hexanes) to yield 16.2 mg of the final product (37.8% yield). ^1H NMR (500 MHz, CDCl_3) δ 0.81 (6H, s, car H-19'), 1.01 (12H, s, car H-16, H-17), 1.42–1.45 (4H, m, car H-2), 1.60–1.63 (4H, m, car H-3), 1.68 (6H, s, car H-20'), 1.70 (6H, s, car H-18), 1.81–1.82 (36H, m, Pc H-1'), 1.95 (6H, s, car H-19), 1.96 (6H, s, car H-20), 1.99–2.00 (4H, m, car H-4), 2.92 (2H, d, J = 15.5, car H-7'), 4.44 (2H, d, J = 15.5, car H-8'), 5.19–5.21 (2H, m, car H-10'), 5.97–5.98 (2H, m, car H-11'), 6.09–6.19 (10H, m, car H-7, H-8, H-10, H-12, H-15), 6.31 (2H, d, J = 15.0, car H-14'), 6.57 (2H, d, J = 12.5, car H-12'), 6.61–6.62 (2H, m, car H-11), 6.65 (2H, d, d, J = 13.5, J = 12.0, car H-15'), 8.44 (4H, d, J = 8.5, Pc H-2(3), H-9(10), H-16(17), H-23(24)), 9.58–9.73 (8H, m, Pc H-1, H-4, H-8, H-11, H-15, H-18, H-22, H-25); MALDI/TOF m/z 1679 (M)⁺, base peak 1238 (M - 441 (carotene))⁺, calc. for $\text{C}_{112}\text{H}_{130}\text{N}_8\text{O}_4\text{Si}$ 1680.4; UV/VIS (CH_2Cl_2) 693-(Pc), 663(Pc), 623(Pc), 468(C), 361(Pc) nm.

Instrumental Techniques. Ultraviolet–visible absorption spectra were measured on a Cary 500 UV–vis–NIR spectrophotometer, and corrected fluorescence excitation and emission spectra were obtained using a Photon Technology International MP-1 spectrofluorometer and optically dilute samples ($A < 0.07$). The excitation spectrum of silicon 1,4,8,11,15,18,22,25-octabutoxyphthalocyanine dihydroxide was used to generate an excitation correction file in the 300–750 nm region by assuming that the absorption and fluorescence excitation spectra were identical.

Femtosecond transient absorption measurements in the visible were carried out with an amplified Ti:sapphire laser system as described earlier.¹⁴ In brief, part of the output of a 1 kHz

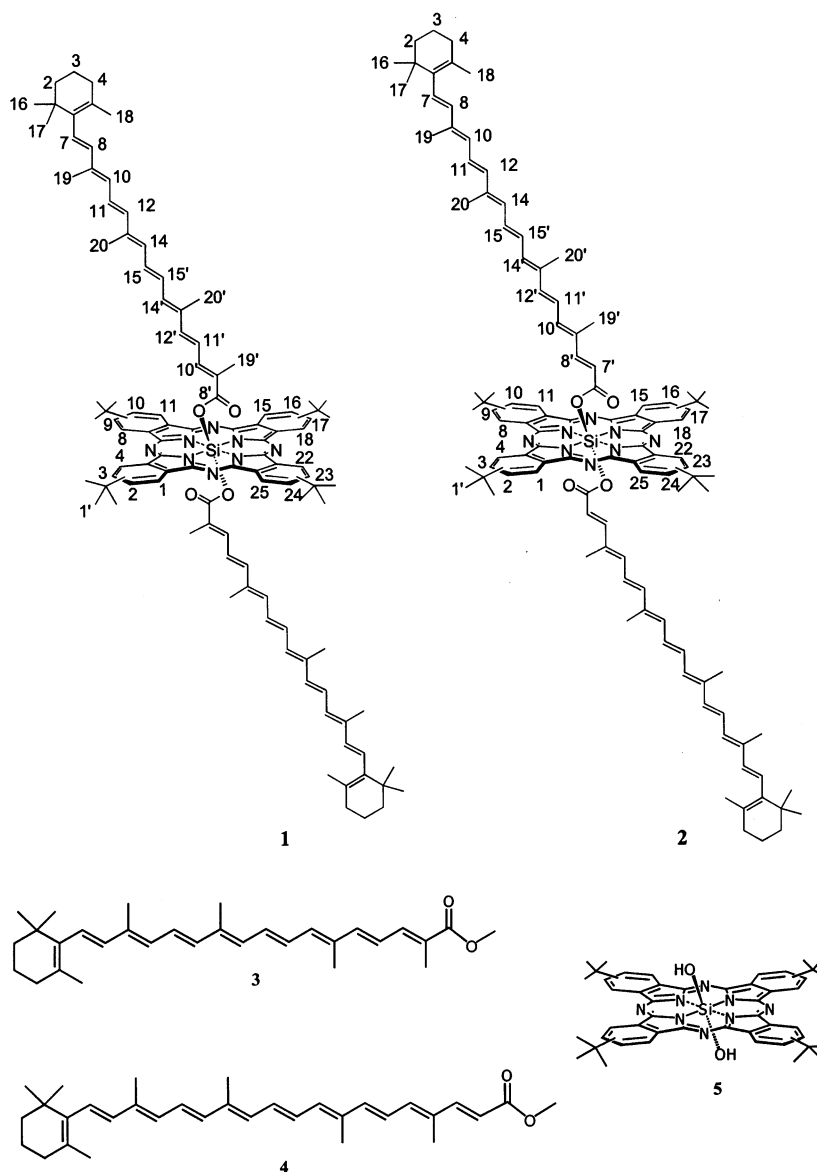


Figure 1. Structures of triads **1** and **2**, model carotenoids **3** and **4**, and phthalocyanine **5**. The three-dimensional structure of **1** and **2** has been inferred by NMR spectroscopy.²⁹

amplified Ti:sapphire laser system (Coherent-BMI α 1000) was used to drive a home-built noncollinear optical parametric amplifier. In the experiments presented here, the excitation wavelength was tuned to 475 nm (17 nm fwhm) so as to selectively excite the S_2 state of the carotenoid. The pulse duration was 80 fs, and the energy was 300 nJ. A white light continuum generated by focusing amplified 800 nm light on a 1 mm sapphire crystal was split into probe and reference. The beams were focused in a 1 mm path-length quartz cuvette to a 150 μ m diameter spot. To avoid sample degradation, the cuvette was mounted on a shaker. The polarization between the pump and the probe was set to the magic angle (54.7°). After passing through the sample, the probe and reference beams were dispersed by a polychromator and projected on a home-built double diode array detector. Femtosecond time delays between pump and probe were controlled by a delay line, covering delays of up to 5 ns.

Femtosecond transient absorption measurements in the IR spectral region were carried out with another amplified Ti:sapphire laser system.³⁴ The laser pulse train was provided by a Ti:sapphire regenerative amplifier (Clark-MXR, model CPA-

1000) pumped by a diode-pumped CW solid-state laser (Spectra Physics, model Millennia V). The typical laser pulse was 100 fs at 790 nm, with a pulse energy of 0.9 mJ at a repetition rate of 1 kHz. Most of the laser energy (80%) was used to pump an optical parametric amplifier (IR-OPA, Clark-MXR). The excitation pulse was sent through a computer controlled optical delay line. The remaining laser output (20%) was focused into a 1.2 cm rotating quartz plate to generate a white light continuum. The continuum beam was further split into two identical parts and used as the probe and reference beams, respectively. The probe and reference signals were focused onto two separated optical fiber bundles coupled to a spectrograph (Acton Research, model SP275). The spectra were acquired on a dual diode array detector (Princeton Instruments, model DPDA-1024).

Data Analysis. The recorded time-resolved spectra were analyzed with a global analysis program using a kinetic model³⁵ consisting of sequentially interconverting species, e.g., $1 \rightarrow 2 \rightarrow 3 \rightarrow \dots$. The arrows indicate successive monoexponential decays of increasing time constants, which can be regarded as the lifetime of each species. Associated with each species is a

lifetime and a difference spectrum, called a species-associated difference spectrum (SADS). The first SADS corresponds to the time zero difference spectrum. In general, the SADS may well correspond to mixtures of excited states and should not be considered to portray spectra of pure states. This procedure enables us to visualize clearly the evolution of the transient states of the system. The instrument response function was fit to a Gaussian (120 fs fwhm) and the group velocity dispersion of the probing white light was fit to a third order polynomial. To optimally illustrate our observations, the SADS are presented instead of raw time-resolved spectra. For selected detection wavelengths, we present raw data by showing the measured kinetic traces including the fit.

3. Results and Discussion

Figure 1 shows the structures of the compounds under study. These include model carotenoid **3**, which comprises 9 carbon-carbon double bonds in its conjugated π -electron system, model carotenoid **4**, which is similar to model carotenoid **3** except that it has 10 conjugated carbon-carbon double bonds, and model phthalocyanine **5**. Conformational information for **1** has been determined by NMR techniques.²⁹ The ^1H NMR spectra of triads **1** and **2** exhibit upshift fields of many of the carotenoid protons due to the phthalocyanine ring currents. In triad **1**, proton 10' is shifted up field to 3.59 ppm from 7.29 ppm in model compound **3**. Triad **2** exhibits also large upfield shifts for protons 7' and 8' (2.92 and 4.44 ppm, respectively), which appear at 5.85 and 7.37 ppm, respectively, in model compound **4**. Upshift fields were also found for the methyl protons 19' and 20' for each triad (in triad **1**, protons 19' and 20' are shifted to -0.21 and 1.41 ppm from 1.99 and 1.97 ppm, respectively, in model **3**; in triad **2**, protons 19' and 20' are shifted to 0.81 and 1.68 ppm from 1.91 and 1.96 ppm, respectively, in model **4**). These field trends are consistent with the proposed three-dimensional structure of **1** and suggest that **2** has a similar structure in which the two carotenoids are covalently attached to the central silicon atom of the phthalocyanine and are oriented almost perpendicular to the tetrapyrrole plane.

Energy Transfer. Absorption and Fluorescence-Excitation Spectra. The absorption spectrum of model phthalocyanine **5** dissolved in *n*-hexane, with an absorption maximum at 671 nm and minor bands at 641, 604, and 355 nm, is shown as the dotted line in Figure 2, parts A and B. This spectrum is typical of a metal phthalocyanine, and only a very weak absorption is observed in the region between 400 and 575 nm. The pattern and spectral positions of the Pc absorption bands very much resemble those of chlorophyll *a*. In triad **1** (solid line, Figure 2A), the addition of the two carotenoid pigments results in a large increase in absorption in the center of the spectrum and a substantial red shift of the phthalocyanine bands, resulting in an absorption maximum of the red-most band at 684 nm instead of 671 nm in model **5**. The absorption of the carotenoid moiety at 466 and 440 nm is slightly blue shifted compared to model carotenoid **3**, which has absorption maxima at 470 and 444 nm (Figure 2A, dashed line). Similar shifts occur in triad **2** (Figure 2B, solid line): the Pc moiety has shifted to the red (684 nm), and the carotenoid moiety has shifted to the blue at 486 and 457 nm, as compared to model carotenoid **4**, which absorbs at 491 and 463 nm (dashed line, Figure 2B).

The fluorescence emission spectrum of the phthalocyanine moiety of triad **1** and **2** (Figure 2, parts A and B, dash-dotted line) has a maximum at 684.7 and a minor band at 759 nm. The figure shows the corrected excitation spectra for the phthalocyanine fluorescence of triad **1** and **2** (solid symbols)

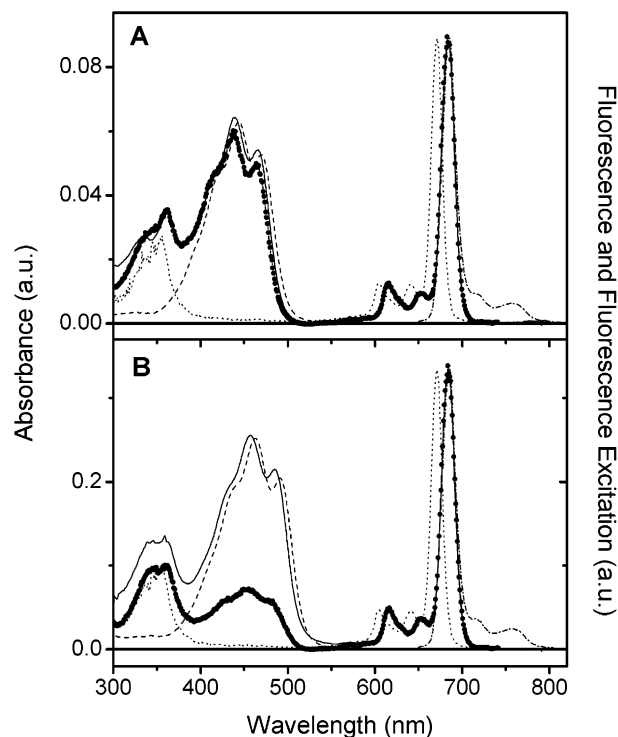


Figure 2. Panel A: absorption spectra of phthalocyanine **5** (dotted line), model carotenoid **3** (dashed line), and triad **1** (solid line); fluorescence spectrum of triad **1** (dash-dotted line); fluorescence excitation spectrum of triad **1** (solid circles). Panel B: absorption spectra of phthalocyanine **5** (dotted line), model carotenoid **4** (dashed line), and triad **2** (solid line); fluorescence spectrum of triad **2** (dash-dotted line); fluorescence excitation spectrum of triad **2** (solid circles).

with emission monitored at 759 nm. The excitation spectrum was normalized to the absorption spectrum at the red-most bands. These spectra clearly indicate a dramatic difference in the singlet-singlet energy transfer efficiency from carotenoid to phthalocyanine: 92% for triad **1** and 30% for triad **2**.

Model Carotenoids 3 and 4: Femtosecond Studies. We first present the femtosecond results from model carotenoid **3** (9 carbon-carbon conjugated double bonds) dissolved in *n*-hexane. We collected time-resolved spectra by exciting the sample with 50 fs flashes at 475 nm and probing with a white-light continuum, with a time range from -3 ps to 200 ps. Rather than presenting the time-resolved spectra themselves, we show the results of a global analysis of these data with a sequential model. Three components were required for an adequate description of the time-resolved data, with lifetimes of 73 fs, 620 fs, and 25 ps (Figure 3A). Each species is characterized by a difference spectrum (so-called SADS) relative to the ground-state absorption, a rise time, and a decay time. The spectrum represents the absorption change, determined from the raw data after correction for the group-velocity chirp in the probe light and deconvolution with the instrument response function. The SADS of the initially created singlet excited S_2 state (red line) shows ground-state bleaching near 480 nm, and a pronounced stimulated emission (SE) at 530 and 570 nm. The lifetime of this state, 73 fs, may be assigned to very rapid internal conversion (IC) from the S_2 to the S_1 state. This S_2 lifetime is almost identical to that reported by Mariño-Ochoa and co-workers²⁹ on the same carotenoid, and appears to be rather short as compared with those of other carotenoids, which are generally on the order of 100–200 fs.^{36–39} The S_2 state evolves into the second SADS (blue line), which has a lifetime of 620 fs. This SADS shows a pronounced excited-state absorption at 545 nm,

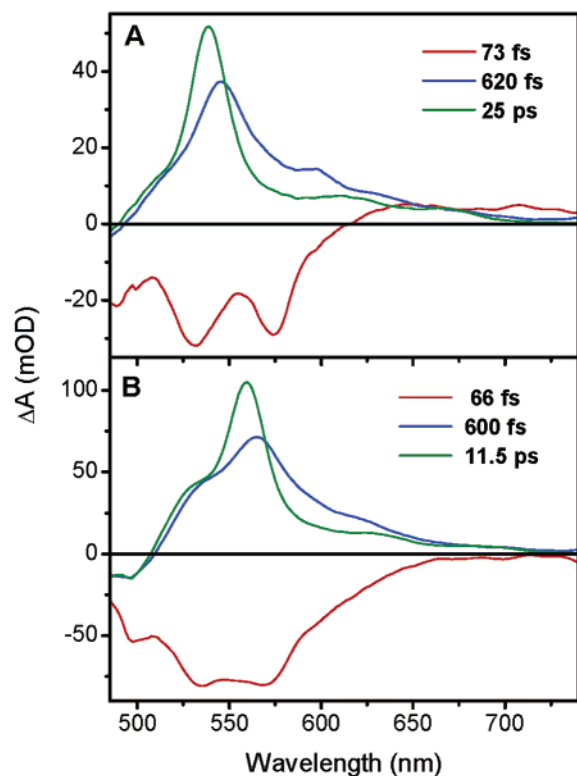


Figure 3. Panel A: Species-associated difference spectra (SADS) that follow from global analysis of the time-resolved experiments on model carotenoid **3** with excitation at 475 nm, with associated lifetimes of 73 fs (red line), 620 fs (blue line), and 25 ps (green line). Panel B: Same as panel A for model carotenoid **4**, with associated lifetimes of 66 fs (red line), 600 fs (blue line), and 11.5 ps (green line).

with shoulders at either side of this maximum, and can be assigned to population of the optically forbidden S_1 state upon IC from S_2 . The third SADS (green line) is formed in 620 fs and has a lifetime of 25 ps. This SADS exhibits an overall blue-shifted and sharpened excited-state absorption with a maximum at 540 nm. The lifetime of the final SADS, 25 ps, results from IC of the S_1 state to the ground state and is similar to the lifetime in solution of other carotenoids with 9 conjugated double bonds, like neurosporene⁴⁰ and violaxanthin.^{41,42}

Figure 3B shows the results of time-resolved measurements on model carotenoid **4** (10 carbon–carbon conjugated double bonds) dissolved in *n*-hexane. As with model carotenoid **3**, three components are required for a satisfactory description of the time-resolved spectra. The first SADS has a lifetime of 66 fs, has a shape very similar to that of the first SADS of model carotenoid **3**, and can be assigned to the S_2 state. The second SADS has a lifetime of 600 fs and exhibits an excited-state absorption near 565 nm with shoulders near 525 and 620 nm. The final SADS has a lifetime of 11.5 ps. It has a blue-shifted absorption with a peak at 560 nm and a shoulder at \sim 530 nm, and we assign it to the S_1 state of the carotenoid. The 11.5 ps lifetime of the S_1 state resembles that of other 10-double bond carotenoids such as spheroidene in solution.⁴³

The spectral evolution of model carotenoids **3** and **4** is similar to those observed earlier for other carotenoids: an extremely short lifetime for the S_2 state in the order of 100 fs, immediately followed by the appearance of an intense absorption that can be attributed to the appearance of the S_1 state. The dynamic blue-shift of the S_1 absorption on the sub-ps time scale is a well-documented phenomenon and has been assigned to a vibrational cooling process in the S_1 state.^{23,44,45}

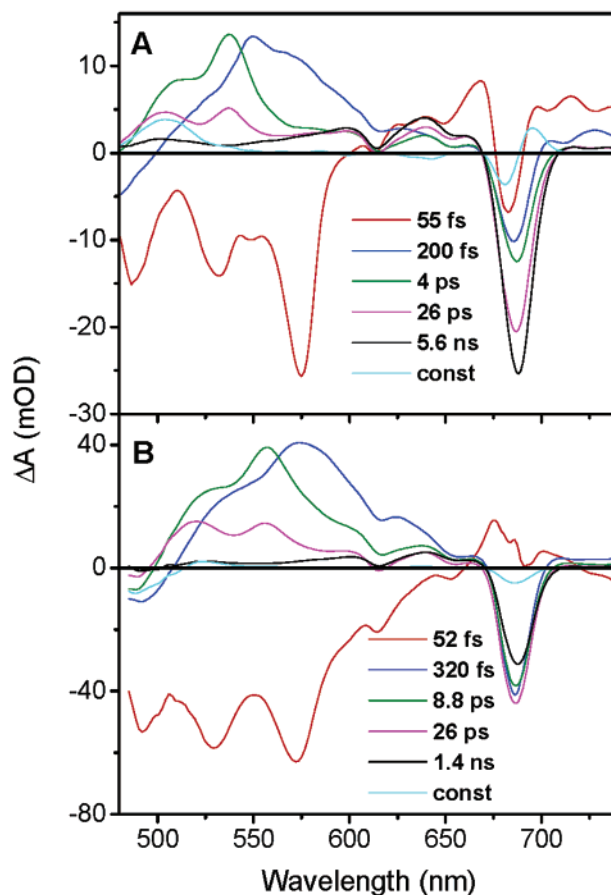


Figure 4. Panel A: Species-associated difference spectra (SADS) that follow from global analysis of time-resolved experiments on triad **1** with excitation at 475 nm, with associated lifetimes of 55 fs (red line), 200 fs (blue line), 4 ps (green line), 26 ps (magenta line), 5.6 ns (black line), and a nondecaying component (cyan line). Panel B: Same as panel A for triad **2**, with associated lifetimes of 52 fs (red line), 320 fs (blue line), 8.8 ps (green line), 26 ps (magenta line), 1.4 ns (black line), and a nondecaying component (cyan line).

Femtosecond Time-Resolved Studies of Triad 1. After dissolving the triads in *n*-hexane, a nonpolar solvent, the light-harvesting function of these systems can be studied in detail, whereas in polar solvents, light-induced electron-transfer processes take place among the carotenoid and Pc moieties of the triads, as we will see below. Figure 4A shows the results of femtosecond time-resolved measurements on triad **1** dissolved in *n*-hexane in the form of a global analysis of the data using a sequential model. In Figure 5, kinetic traces are depicted at selected wavelengths (circles), along with the results of the global analysis procedure (solid lines). To illustrate the quality of the data, a selection of 12 raw time-resolved spectra out of the total of 120 recorded spectra is shown in Figure 9B of the Appendix. After excitation, optically dark states of the carotenoids are rapidly generated, giving rise to absorption features that are red-shifted with respect to that of the ground state of the carotenoid. The various carotenoid electronic excited states exhibit dynamics on a number of time scales and may be involved in IC processes and EET to Pc. The latter process becomes apparent in the spectral evolution by changes in the ground-state bleaching and SE of phthalocyanine near 685 nm. No less than six kinetic components are required for satisfactory description of the time-resolved spectra. The SADS of the initially created excited state (red line) has a lifetime of 55 fs. It exhibits a pronounced negative signal from 480 to 600 nm, arising from ground-state bleaching of the carotenoid near 480

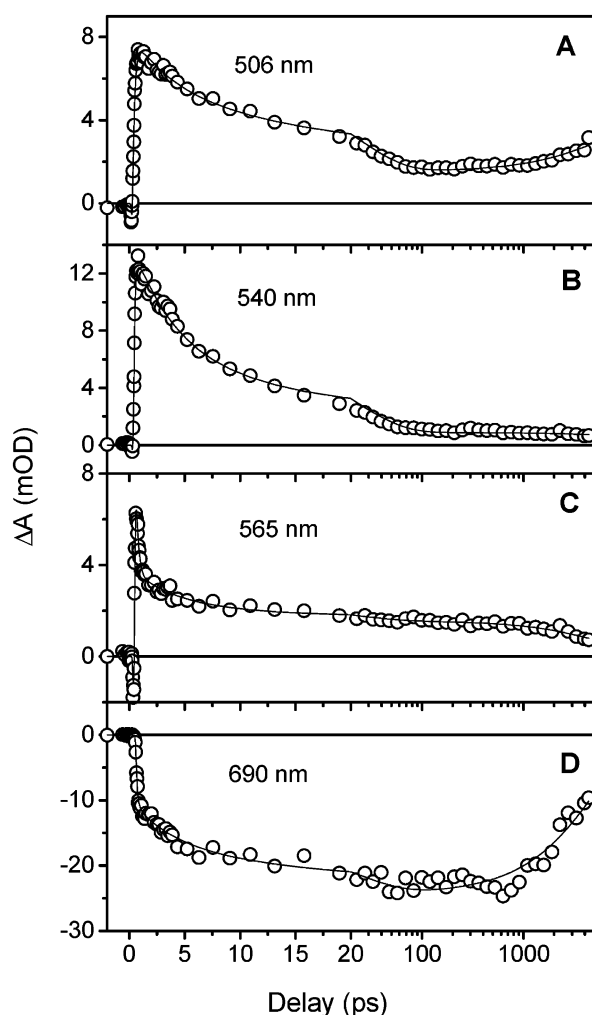


Figure 5. Kinetic traces measured in triad **1** at (A) 506 nm, (B) 540 nm, (C) 565 nm, and (D) 690 nm with excitation at 475 nm. The solid lines denote the fitted curves as determined by the global analysis procedure, of which the SADS are displayed in Figure 4A.

nm and stimulated emission to the ground state from ~ 520 to 600 nm. In addition, the initial SADS shows a band-shift like signal in the Q_y region of the Pc, which may be assigned to an electric-field effect by the charge redistribution of the excited carotenoid on the absorption spectrum of Pc. We assign this component to the population of the strongly allowed S_2 state of the carotenoid. The second SADS (blue line) has a lifetime of 200 fs. It shows a broad absorption near 550 nm and a negative feature near 685 nm. The negative signal at 685 nm can be attributed to ground-state bleaching and SE of Pc, which indicates that energy transfer has taken place from the S_2 state of the carotenoid to the Pc. This becomes apparent in the kinetic trace at 690 nm in Figure 5D as an almost instantaneous partial rise of the negative bleach/SE signal. The absorption near 550 nm can be assigned to population of the S_1 state of the carotenoid, which is formed through internal conversion from the S_2 state. The spectral maximum and the shape (blue line) are very similar to that of the second SADS of the model carotenoid, indicating that this state corresponds to a vibrationally hot S_1 state of the carotenoid, although its lifetime appears to be significantly shorter (200 vs 600 fs). The 200 fs dynamic process in the S_1 state is manifested in the kinetic trace at 565 nm, where a rapid decay of the absorption signal by about 40% is observed. The third SADS (green line) has a lifetime of 4 ps, and shows an absorption maximum near 540

nm. The spectral characteristics of this SADS encompass a blue shift with respect to the previous SADS (blue line). Importantly, the third SADS shows a pronounced shoulder near 505 nm. This absorption feature is not observed in the 9-double bond model carotenoid in solution (Figure 2). An induced absorption band that is blue-shifted with respect to that of S_1 and coincides with that of the carotenoid triplet state (see also below) is typical for the presence of the S^* state.^{18,23,46} The fourth SADS (magenta line) has a lifetime of 26 ps. It shows a significant decrease of the S_1 absorption at 540 nm and a concomitant rise of the Pc bleach/SE with respect to the previous SADS (green line). The S^* absorption near 505 nm has decayed to a much smaller extent, which indicates that this state has a significantly longer lifetime than the S_1 state, as observed previously in several bacterial LH complexes and in spirilloxanthin in solution.^{18,23} The separate lifetimes of S_1 and S^* are illustrated in the kinetic traces in Figure 5, parts A and B, where S^* (506 nm) clearly decays more slowly than S_1 (540 nm). The fifth SADS (black line) has a lifetime of 5.6 ns and its main feature involves a bleach/SE band near 690 nm. The time range used in this experiment (4.5 ns) is too short to accurately determine this time constant, and the 5.6 ns lifetime has been taken from single-photon timing experiments on the same triad (not shown) and fixed in the global analysis routine. We remark that, if this lifetime is allowed to vary in the global analysis routine, a very similar lifetime of 4.8 ns is obtained. The SADS is relatively flat in the 480–600 nm region, showing that the vast majority of carotenoid singlet states, e.g., S_1 and S^* , have disappeared after 26 ps, and only Pc singlet excited states are present with bleaching/SE at 685 nm, a broad, flat absorption at longer wavelengths and a small bleach of the Q_x band at 615 nm. The final, nondecaying SADS (cyan line) shows the rise of a marked absorption band at 505 nm, indicative of formation of the carotenoid triplet state. This is clearly seen in the kinetic trace at 506 nm (Figure 5A), where the signal passes through a minimum near 100 ps and rises thereafter. Concomitantly, the ground-state bleach/SE signal on the Pc near 685 nm in the nondecaying SADS has disappeared completely and has been replaced by a band shift-like signal.

The spectral evolution in triad **1** shows similarities to that of the model carotenoid, but also shows marked differences that can be related to the covalent attachment to the Pc. First of all, the lifetime of the optically allowed S_2 state is shorter in triad **1**, 55 fs, as compared to the model carotenoid, 73 fs. The SADS in Figure 4 show that, in 55 fs, a ground state bleaching/SE band of Pc evolves from the band-shift like signal (red to blue line). These observations indicate that energy transfer to the Pc occurs from the optically allowed S_2 state of the carotenoid.

In competition with the energy transfer process, the S_2 state decays by internal conversion to low-lying optically forbidden carotenoid singlet excited states. Upon decay of the S_2 state, a broad absorption near 550 nm associated with the S_1 state appears, which shifts to the blue with a time constant of 200 fs (blue to green lines, Figure 4A). The spectral evolution is very similar to that arising from the vibrational cooling process in model carotenoid **3**, occurring with a time constant of 600 fs. The increased cooling rate in triad **1** most likely follows from an enhanced vibronic coupling in the triad because of the covalent linkage to the Pc, which opens up more degrees of freedom for intramolecular vibrational relaxation. Concomitant with the blue shift of the carotenoid S_1 absorption, we observe a slight increase and red shift of the bleach/SE signal near 690 nm. The rise of the bleach/SE signal possibly results from energy transfer from the vibrationally excited S_1 state of the carotenoid

to Pc. However, internal conversion from the Q_x to Q_y state of the Pc or a dynamic solvation process of the Pc Q_y states in the hexane solvent may also contribute to these signals.

The induced absorption band near 540 nm, which can be assigned to the relaxed S_1 state, has a lifetime of 4 ps, significantly shorter than that of model carotenoid **3** (25 ps). The concomitant rise of the Pc bleach/SE near 690 nm indicates that this shortening of the S_1 lifetime results from energy transfer to Pc (green to magenta line). Given an IC time constant of 25 ps of the S_1 state, it follows that, upon its formation, the S_1 state transfers its energy to Pc with a rate of $(4.7 \text{ ps})^{-1}$, at an efficiency of 84%.

The induced absorption near 505 nm is a new, unexpected feature that becomes apparent after vibrational relaxation of the S_1 state. We assign the 505 nm ESA to formation of the S^* state, a new carotenoid singlet excited state which we have recently characterized in carotenoids bound to bacterial LH complexes and in the long carotenoid spirilloxanthin in hexane solution.^{18,23,46} The S^* state has a lifetime of 26 ps in triad **1**. The accompanying rise of the phthalocyanine bleaching near 690 nm with this time constant indicates that S^* transfers energy to Pc.

The time-resolved data for triad **1** allow for an assessment of the relative contributions by the various carotenoid electronic excited states to the energy transfer process to Pc. From the S_2 lifetimes of model carotenoid **3** and triad **1**, it follows that the S_2 channel accounts for about 30% of the total energy transferred to Pc. This agrees reasonably with the relative bleach/SE signal of the Pc after S_2 relaxation (Figure 4A, blue line), which has an amplitude of 40% compared to that after all energy transfer processes are complete (black line). The rise of the Pc bleach/SE signal furthermore indicates a possible minor contribution of $\sim 8\%$ by the vibrationally excited S_1 state (blue to green line), a major contribution of $\sim 32\%$ by the relaxed S_1 state (green to magenta line), and a significant (20%) contribution by the S^* state (magenta to black line). The light harvesting function of carotenoids in triad **1** shows striking similarities to that of the LH2 complex of *Rb. sphaeroides*, where a similar use of S_2 , hot S_1 , S_1 , and S^* pathways leads to a 90% total carotenoid–BChl energy transfer efficiency.²³

With regard to the roles of the S_2 and S_1 states the present results agree quite well with earlier findings on the same compound.²⁹ Virtually the same S_2 lifetimes were found for triad **1** and model carotenoid **3**, whereas an S_1 lifetime of 2.8 ps was reported, which differs slightly from the number in this study (4 ps). Moreover, Mariño-Ochoa et al. found no evidence for energy transfer processes on time scales longer than 2.8 ps. The reason for this is not entirely clear, but we note that the experiments of Mariño-Ochoa et al. were conducted on triad **1** in a different solvent (toluene) on a short time axis of 20 ps and that, in the present experiment, the 4 ps lifetime is estimated from a full spectral analysis of a broad dataset encompassing carotenoid and Pc excited-state features, rather than from single kinetic traces.

Femtosecond Time-Resolved Studies of Triad 2. The results for triad **1** indicate how the manifold of excited states in carotenoids are involved in singlet energy transfer processes to phthalocyanine. To assess the role of the excited-state energies of carotenoids on energy transfer rates and efficiencies in a similar geometrical configuration, we have performed fs transient absorption experiments on triad **2**, which binds a pair of carotenoids with 10 carbon–carbon double bonds each, as shown in Figure 1. Figure 4B shows the results of a global analysis of the femtosecond time-resolved measurements on triad

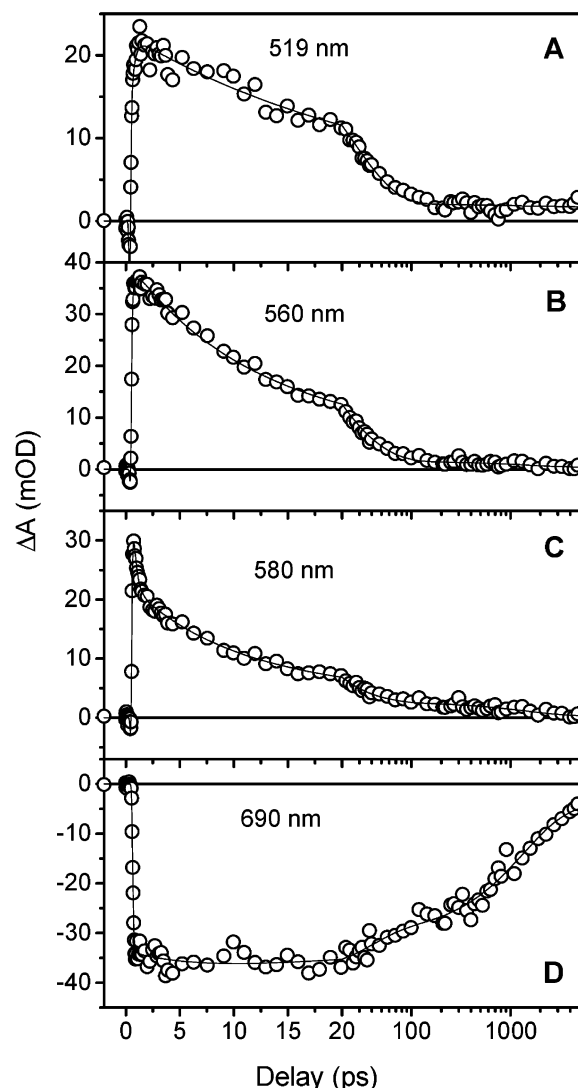


Figure 6. Kinetic traces measured in triad **2** at (A) 519 nm, (B) 560 nm, (C) 580 nm, and (D) 690 nm with excitation at 475 nm. The solid lines denote the fitted curves as determined by the global analysis procedure, of which the SADS are displayed in Figure 4B.

2 in *n*-hexane upon excitation at 475 nm. Kinetic traces at selected wavelengths have been depicted in Figure 6 (circles), along with the result of the global analysis (solid lines). Figure 9A of the Appendix shows a selection of raw time-resolved spectra. As with triad **1**, 6 components are needed for a satisfactory description of the time-resolved data. The first SADS (red line, Figure 4B) has a lifetime of 52 fs and can be assigned to the initially excited S_2 state of the carotenoid and exhibits distinct ground-state bleaching and stimulated emission features from 480 to 620 nm and a band-shift like feature around 680 nm superimposed on an induced absorption. The second SADS (blue line) has a lifetime of 320 fs and shows a pronounced induced absorption at 570 nm, which we attribute to the vibrationally excited S_1 state of the carotenoid. It furthermore shows a bleach/SE signal near 690 nm, which results from very rapid energy transfer to Pc from the carotenoid S_2 state, as evidenced by the rapid rise of a bleach/SE signal of the kinetic trace at 690 nm (Figure 6D). The third SADS (green line) has an associated decay time of 8.8 ps. It shows an induced absorption at 555 nm and pronounced shoulder near 525 nm. In analogy with triad **1**, we assign the former feature to the thermally relaxed S_1 state of the carotenoid and the latter to the S^* state. Thus, upon carotenoid excitation, the S^* state is

transiently present not only in triad **1** but in triad **2** as well. The system further evolves into the fourth SADS (magenta line), which has a lifetime of 26 ps. As compared to the previous SADS, a slight increase of the bleach/SE signal of Pc takes place in the 690 nm region. Concomitantly, the absorption at 555 has largely disappeared, indicating a decay of the S_1 state. The S^* absorption at 520 nm has largely stayed intact, similar to the situation in triad **1**. The distinct lifetimes of S_1 and S^* become apparent in the kinetic traces at 519 (Figure 6A) and 560 nm (Figure 6B). The fifth SADS (black line) has a lifetime of 1.4 ns. Given its flat absorption in the 480–600 nm region and the bleach/SE band at 685 nm, we attribute this spectrum solely to the singlet excited state of Pc. Intriguingly, the amplitude of the bleach/SE band of Pc has decreased by about 25% as compared to the previous SADS, denoting a quenching of Pc singlet excited states in the 26 ps evolution to this state.

Moreover, the singlet excited state of Pc, which lives 1.4 ns, appears to be quenched as compared to model Pc **5** (5.23 ns) and to Pc in triad **1** (5.6 ns). The reasons for these Pc singlet state quenchings are not clear, but they hint at direct singlet-state quenching mechanisms by carotenoids. Further experimental study and discussion of this phenomenon will be the subject of a forthcoming paper. The final, nondecaying SADS (cyan line) shows a small negative feature in the Pc bleaching region. This may be assigned to a small residue of singlet excited states of Pc, as single photon timing experiments on triad **2** yielded a biexponential decay of the Pc singlet state with time constants of 1.4 and 4 ns (not shown). In the present experiments, the time axis (4.5 ns) is not sufficient to distinguish the latter lifetime from a nondecaying component. Although the Pc triplet yield in triad **2** will be significantly lower as compared to that of triad **1** as a result of the quenched singlet lifetime, the final SADS may have a contribution by Pc triplet states which have formed through intersystem crossing from the Pc singlet state. It is important to note, however, that the biexponential decay of the Pc excited states precludes an accurate estimate of the final SADS, and it is thus difficult to interpret the data in terms of molecular processes that occur in this time range.

Despite the fact that the carotenoid to Pc energy transfer efficiency is dramatically lower in triad **2** as compared to that for triad **1**, the overall spectral evolution upon carotenoid excitation is very similar in these two systems: the same number of kinetic components is needed, and the difference spectra of the electronic states involved exhibit essentially the same absorption features. The total Pc bleach/SE amplitude near 685 nm in triad **2** remains significantly lower at all times as compared to that of triad **1**, consistent with the lower energy transfer efficiency from the carotenoids to the Pc.

Energy transfer from the optically allowed carotenoid S_2 state to the Pc moiety appears to proceed at a rate similar to that in triad **1**, as the S_2 lifetimes are very similar (55 and 52 fs), as are the S_2 lifetimes of their model compounds (73 and 66 fs). The quantum yields of energy transfer from S_2 in **1** and **2** can be estimated to be approximately 30% and 25%. The difference in energy transfer efficiency between triad **2** and triad **1** finds its origin in the properties of the optically forbidden states S_1 and S^* . The lifetime of the S_1 state, 8.8 ps in triad **2**, is only marginally shorter than that of model carotenoid **4**, 11.5 ps. This indicates that only a little energy transfer occurs from the S_1 state in triad **2**. From its lifetime, an energy transfer rate constant of $(37 \text{ ps})^{-1}$ can be deduced, which implies that only 23% of the S_1 states that are formed transfer their energy to Pc. In agreement with this, the bleach/SE signal of Pc increases

only slightly upon decay of the S_1 state (Figure 4B, green to magenta line evolution). Thus, energy transfer from the carotenoid to Pc in triad **2** proceeds almost exclusively through the S_2 state. This situation is very reminiscent of photosynthetic antenna systems that show similarly low carotenoid to (B)Chl transfer yields, like the LH1 complex of *Rs. rubrum*¹⁸ and the CP43 and CP47 core antenna proteins of Photosystem II.¹⁹

Energy Transfer from the S_1 State in Triads 1 and 2. It has become increasingly clear that efficient light harvesting strategies by carotenoids involve the employment of the optically forbidden S_1 state as an excited-state energy donor. Although it was previously believed that an electron exchange mechanism could mediate the energy transfer process, it was recently shown by quantum chemical methods that in natural light-harvesting complexes the exchange term is insignificant compared to the Coulombic interactions.^{16,17} Energy transfer from the S_1 state to (B)Chl was, in many cases, found to proceed on the picosecond time scale, which implies a significant electronic coupling of the order of 10^3 of cm^{-1} .^{12–14} How an optically dark state can exhibit such a strong Coulombic coupling is far from clear: it was argued that it follows from higher order terms in the multipole expansion of the transition charge density, and it was suggested that the exact geometric details of donor and acceptor influence this coupling to a great extent.^{16,17,47} On the other hand, we have preliminary data on a model carotenoid–gold porphyrin dyad in which triplet–triplet energy transfer from a cyclic tetrapyrrole to an attached carotenoid occurs in ~ 1 ps (Kodis et al., unpublished). This indicates that exchange-mediated processes can occur on the ps time scale and therefore should not be ruled out for S_1 transfer in the covalently linked artificial antenna systems.

Triads **1** and **2** show vastly different energy transfer rates from their respective S_1 states to Pc, of $(4.8 \text{ ps})^{-1}$ and $(37.5 \text{ ps})^{-1}$, respectively. Given the similar geometric structures of triads **1** and **2**, this phenomenon is likely associated with the relative energy levels of the S_1 states in these systems. Although we do not know the S_1 energy levels of model carotenoids **3** and **4**, approximate estimates may be made from comparison with carotenoids that have the same number of conjugated double bonds. For neurosporene, which has 9 double bonds, the 0–0 transition of the S_1 state has been estimated to lie around 654 nm (15300 cm^{-1}).⁴⁸ For violaxanthin (9 double bonds), estimates range from 672 (14880)⁴⁹ to 691 nm (14470 cm^{-1}).⁴¹ For spheroidene (10 conjugated double bonds), estimates of the 0–0 transition of the S_1 state lie between 704 (14200)⁴⁸ and 746 nm (13400 cm^{-1}).⁵⁰

To illustrate the effect of a decreasing energy gap (10 vs 9 bond carotenoid) on the spectral overlap of donor and acceptor, in Figure 7, we have depicted the S_1 emission of neurosporene (dashed line) and spheroidene (dotted line), both taken from ref 48, along with the absorption of the Pc moiety in triads (solid line). Obviously, the S_1 emission from the 9-conjugated double bond carotenoid is in much better resonance with Pc than that of the 10-conjugated-double-bond carotenoid, with a 3-fold larger spectral overlap of neurosporene as compared to spheroidene. We note that the carotenoid S_1 energies are somewhat controversial in the sense that near-IR transient absorption spectroscopy systematically yields results that are lower by $400\text{--}800 \text{ cm}^{-1}$ on the same carotenoids compared to fluorescence spectroscopy.⁵⁰ If we assume such a red-shift by $400\text{--}800 \text{ cm}^{-1}$ of the S_1 emission, the differences in spectral overlap between triad **1** and triad **2** become even larger because the 10-double-bond carotenoid shifts almost completely out of the overlap region with the Pc absorption, whereas the 9-double

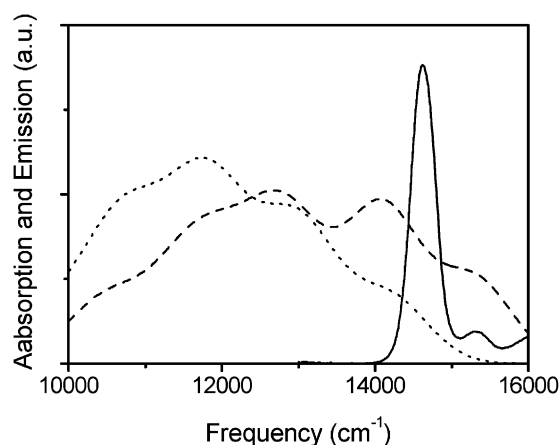


Figure 7. Absorption spectrum of phthalocyanine bound to triad **1** or **2** (solid line), fluorescence from the S_1 state of neurosporene, a 9 conjugated carbon–carbon double bond carotenoid (dashed line), and spheroidene, a 10 conjugated carbon–carbon double bond carotenoid (dotted line), taken from ref 48. The vertical scaling of absorption and emission spectra is arbitrary. See text for details.

bond carotenoid does so to a much smaller extent. Thus, it may be concluded that the spectral overlap of donor and acceptor states is to a significant extent responsible for the large difference in carotenoid light harvesting efficiency from the S_1 state in triad **1** and **2**.

S^* State in Triads **1 and **2**.** The spectral evolution following carotenoid excitation in both triads **1** and **2** clearly indicates that, in addition to S_2 and S_1 , the recently characterized S^* state is transiently formed. Thus far, the S^* state has been observed in spirilloxanthin in solution and in carotenoids bound to bacterial light harvesting complexes.^{18,23,46} Gradinaru et al. and Papagiannakis et al. have previously reported that S^* is populated in parallel with S_1 through IC from S_2 and have speculated that specific pigment–protein interactions could induce formation of this state in carotenoids shorter than spirilloxanthin.^{18,23,46} The present observation of S^* in an artificial antenna complex indicates that carotenoid–protein interactions are not necessary for the formation of this state. Moreover, we did not detect transient absorption characteristic of S^* in model carotenoids **3** and **4** indicating that either S^* is not populated in the model carotenoids or it quickly relaxes to the S_1 state and thereby escapes detection. These observations suggest that formation, or perhaps kinetic stabilization of S^* , results from electronic (vibrational) coupling with nearby pigments. The sizable amplitudes of the S^* absorption bands at 505 (triad **1**) and 520 nm (triad **2**) indicate that S^* is formed in significant amounts. Although the extinction coefficients of these bands are not known, an estimate of the population of S^* can be made from the relative energy transfer fraction in triad **1**: S^* contributes about 20% of the total energy from the carotenoid to Pc (Figure 4A), and, given the fact that the energy transfer efficiency is almost 100%, about 20% of the photo-excited carotenoids in triad **1** must relax to the S^* state. Assuming that the extinction coefficients of the S^* bands in triads **1** and **2** are similar, we conclude from the amplitude of the S^* bands (magenta lines in Figure 4A and B) that the transient S^* concentration in triad **2** is similar, i.e., about 20%.

Strikingly, S^* has identical lifetimes in triads **1** and **2** of 26 ps, suggesting that, in contrast to the S_1 state, the lifetime of S^* does not depend strongly on the conjugation length of the carotenoid by an energy-gap law dependence. However, in triad **1**, the decay of S^* is associated with a rise of the Pc bleach/SE signal (Figure 4A). In the absence of other carotenoid excited

states on this time scale, this observation strongly indicates that S^* transfers energy to Pc. The situation in triad **2** is completely different. The Pc bleach/SE signal does not rise concomitantly with the decay of S^* in 26 ps but, instead, shows a marked decay by about 25% (Figure 4B).

Our results are consistent with the previous interpretation that S^* corresponds to one of the theoretically predicted optically forbidden covalent states $^1B_u^-$ or $^3A_g^-$.^{18,23,46} Another possibility, if the simultaneous decay of S^* and the singlet excited state of Pc in triad **2** is not fortuitous, is that this new transient feature corresponds to a collective excited state of the triad. If this is the case, in triad **1**, the composite state relaxes to populate the singlet excited state of Pc, whereas in triad **2**, presumably for thermodynamic reasons, it does not and decays by IC to the ground state. Interestingly, Polivka et al. reported the transient formation of carotenoid radicals in the LH2 complex of *Rb. sphaeroides* with a lifetime identical to that of S^* in the same complex⁵¹ which suggests that S^* could possess a certain degree of charge-transfer character and might represent a state that is more complex than previously thought.

Andersson and Gillbro⁵² and Yoshizawa et al.⁵³ reported transient absorption features similar to the S^* state in polyenes homologous with all-*trans*- β -carotene having 13, 15, and 19 conjugated double bonds and assigned these features to the hot carotenoid ground state. However, the shape of the difference spectrum of S^* and its role in ultrafast triplet formation and light harvesting rules out this possibility.^{18,23} Moreover, as a result of the differences in light-harvesting efficiencies, significantly more excited-state energy is dissipated to the carotenoid ground state in triad **2** as compared to triad **1** on the picosecond time scale. Despite this, the amplitude of the S^* signals in triads **1** and **2** are very similar, which provides another argument against the interpretation of S^* as a hot carotenoid ground state.

Recent femtosecond stimulated Raman experiments have suggested that, in short carotenoids (<12 conjugated double bonds), incomplete vibrational relaxation takes place during the S_1 lifetime, whereas in long carotenoids (>12 double bonds), the S_1 state may rapidly relax to its 0–0 level.^{53,54} In this scenario, S^* could be identified with the fully relaxed S_1 state. In shorter carotenoids, the S^* or fully relaxed S_1 state is only observed when the carotenoid is interacting with chlorophylls in LH systems or with Pc in the artificial systems. In this view, the tetrapyrrole states could act as mediator states allowing the carotenoid to reach the zero vibration level of S_1 . Slow relaxation in the lower vibrational states of the singlet manifold could explain why different spectroscopic methods give different values for the 0–0 transition of the S_1 state in carotenoids.^{41,48–50} However, picosecond time-resolved anti-Stokes Raman experiments have shown that complete vibrational relaxation in β -carotene is complete in less than 2 ps, arguing against the picture painted above.⁵⁵ Moreover, application of femtosecond stimulated Raman spectroscopy on carotenoids by several research groups has not yet given mutually consistent results^{53,54,56,57} and the validity of Yoshizawa's results remains to be demonstrated.

In triads **1** and **2**, the SADS that represents the absorbance changes after S^* has decayed show a relatively flat absorption in the 480–550 nm region (Figure 4, parts A and B, black line), arising from the Pc singlet excited state. This indicates that no detectable carotenoid triplet states are directly generated from S^* , in contrast to the case of the LH complexes of photosynthetic bacteria, where the S^* state is a precursor to the picosecond formation of carotenoid triplet states. These carotenoid triplets may be formed with a yield of up to 30% by a singlet fission

mechanism.^{18,23,46} It thus appears that in triads **1** and **2** the singlet fission mechanism is either not active or so slow that it cannot compete with other relaxation processes from S^* including energy transfer to Pc in triad **1**. Quantum-chemical calculations by Tavan and Schulten^{24,28} have shown that the “covalent”, optically dark excited singlet states in carotenoids exhibit a doubly excited triplet character, and they suggested that dissociation, or fission, of such states into pairs of spin-correlated triplet states could be induced by lattice distortions, i.e., structural deformations of the polyene backbone. In full agreement with this, recent experiments on carotenoid-reconstituted LH complexes *Rb. sphaeroides* R.26 and *Rs. rubrum* have demonstrated that the extent of triplet generation from S^* depends on the degree of protein-imposed structural distortion of the polyene backbone in the LH complex.⁴⁶ In the triads, the carotenoids assume a relaxed, planar conformation (Figure 1), which minimizes the fission probability and suppresses triplet formation.

Triplet Energy Transfer in Triads 1 and 2. In triad **1**, formation of the carotenoid triplet state immediately follows decay of the Pc singlet excited state with a time constant of 5.6 ns, as indicated by the rise of the triplet absorption at 505 nm (Figure 4A, sixth SADS, cyan line). The Pc triplet state, which is formed through intersystem crossing from the Pc singlet excited state, is not observed at any time in the spectral evolution. This implies that triplet–triplet energy transfer from the Pc to the carotenoid takes place very rapidly, and proceeds at a rate that is much faster than the rate of Pc singlet state decay, $(5.6 \text{ ns})^{-1}$, which itself is the sum of the radiative rate, the ISC rate, and the IC rate. This observation is consistent with recent experiments on a carotenoid–goldporphyrin (C–AuP) dyad alluded above, where it was shown that the AuP triplet excited state, formed from the singlet excited state in 560 fs, was quenched from 2.4 ns to 1.5 ps by triplet–triplet energy transfer to yield the carotenoid triplet excited state [Kodis et al., unpublished results]. Time constants on the order of 10 ns have been reported for BChl to carotenoid triplet transfer in bacterial light harvesting complexes.⁵⁸ It thus appears that the triplet–triplet energy transfer process in triad **1** is orders of magnitude faster than in natural photosynthetic systems. This may be related to the covalent linkage between the carotenoid and Pc moieties in the triad, which provides closer contacts for exchange mediated processes between the π orbitals of the donor and acceptor than the van der Waals contacts between (B)Chls and carotenoids in the natural photosynthetic systems.

Our experiments do not give clear-cut information on the triplet energy transfer processes in triad **2**; the Pc singlet state is quenched as compared to triad **1**, which accordingly lowers the Pc triplet yield. Moreover, the multiexponential decay of Pc on the nanosecond time scale severely hampers an assessment of late-time spectra, which contain the dynamic information regarding formation of the carotenoid triplet state.

Electron Transfer. *Cyclic Voltammetry.* Upon dissolving triads **1** and **2** in polar solvents, light-induced electron-transfer events occur among the carotenoid and Pc moieties. Electrochemical measurements were undertaken to investigate the redox properties of phthalocyanine and carotenoid moieties in triads **1** and **2**. These were necessary in order to estimate the energies of the charge-separated states. The measurements were carried out with a Pine Instrument Co. model AFRDE4 potentiostat at ambient temperatures with a glassy carbon or platinum wire working electrode, a Ag/Ag⁺ reference electrode, and a platinum wire counter electrode. Measurements were performed in benzonitrile containing 0.1 M tetra-*n*-butylammonium hexafluor-

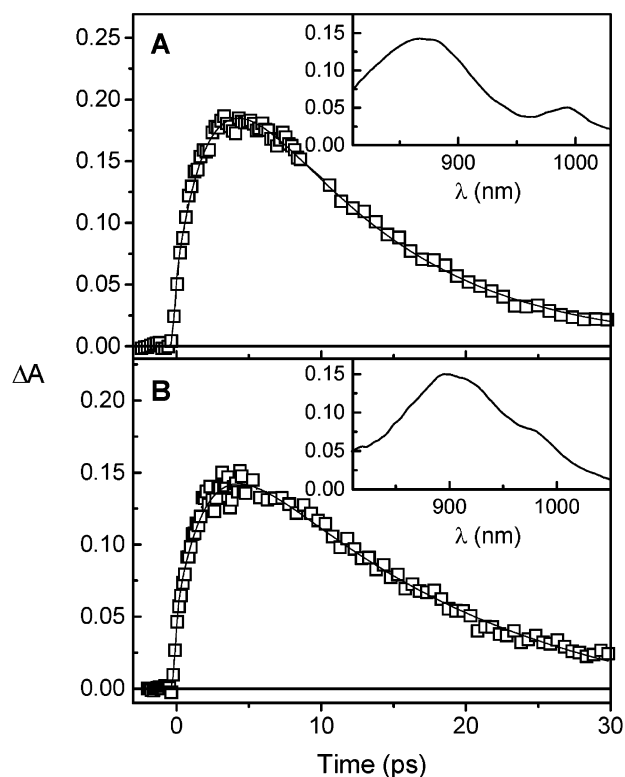


Figure 8. A: Kinetic trace recorded in triad **1** dissolved in benzonitrile upon excitation at 680 nm, and detection at 870 nm. The inset shows the absorbance difference spectrum at a delay of 2 ps under the same conditions. B: Same as A for triad **2**, with detection at 900 nm. The inset shows the absorbance difference spectrum at a delay of 3 ps under the same conditions.

rophosphate and ferrocene as an internal standard (oxidation at 0.46 V vs SCE). Phthalocyanine model **5** featured an oxidation wave at 1.04 V vs SCE and reduction at -0.76 V vs SCE. Model carotenoid **3** (9 double bonds) showed an oxidation wave at 0.68 V vs SCE, and 10 double bond carotenoid model **4** showed an oxidation wave at 0.60 V vs SCE, both irreversible. Triads **1** and **2** were found to exhibit a ~ 0.02 V higher oxidation potential of their carotenoid moieties (0.7 and 0.62 V vs SCE) and ~ 0.04 V lower reduction potential of phthalocyanine (-0.72 V vs SCE). The energies of the $C^{\bullet+}$ – $Pc^{\bullet-}$ charge-separated states in triads **1** and **2** were estimated as 1.42 and 1.34 eV, respectively, based on the electrochemically determined oxidation and reduction potentials of the triads.

Femtosecond Transient Absorption. The formation of a $C^{\bullet+}$ – $Pc^{\bullet-}$ charge separated state by photoinduced electron transfer was probed by a fs transient absorption spectroscopic investigation of the triads in benzonitrile solution. In both triad **1** and triad **2**, $C^{\bullet+}$ – $Pc^{\bullet-}$ charge separation was observed. This state can be readily identified by the phthalocyanine radical anion near 580 and 990 nm and/or by the carotenoid radical cation absorption at 820–950 nm (see Figure 8A,B inset). Figure 8A shows the kinetic trace of triad **1** with excitation at 680 nm and detection at 870 nm and the time-resolved difference spectrum obtained after 2 ps (inset). At 680 nm, the excitation light is absorbed exclusively by the Pc moiety generating the singlet excited state which decays with a time constant of 2.5 ps to yield the $C^{\bullet+}$ – $Pc^{\bullet-}$ charge-separated state, observed as a rise/formation of the carotenoid radical band at 870 nm. The charge-separated state decays to the ground state with a lifetime of 10.5 ps.

Figure 8B shows the corresponding kinetic trace for triad **2**, with detection at 900 nm. The time-resolved spectrum, obtained

after 3 ps, is shown in the inset. In this case, the $C^{+}-Pc^{-}$ charge-separated state is formed with a time constant of 2.2 ps and decays to the ground state in 17 ps. Electrochemical measurements gives a value of the $C^{+}-Pc^{-}$ charge-separated state energy that is ~ 0.1 eV higher for triad **1**. Therefore, there is less driving force for electron transfer in this case and charge separation is slower, whereas charge recombination is faster compared to triad **2**. The induced absorption due to the carotenoid radical cation in triad **2** is shifted to the red relative to that in **1**, as is expected.

In *n*-hexane, charge separation was not observed, most likely due to lack of charge stabilization in the nonpolar solvent.

4. Conclusions

The application of time-resolved spectroscopy to triads **1** and **2** has revealed that carotenoids and tetrapyrroles can be designed in a compact architecture to closely mimic light-harvesting and photoprotective functions as they exist in natural photosynthesis. Triad **1**, which binds a pair of carotenoids with 9 carbon–carbon conjugated double bonds, is a most appealing example because it exhibits near complete light-harvesting through three of the available electronic states of the carotenoid: the optically allowed S_2 state, the optically forbidden S_1 state, and the newly discovered S^* state. In contrast to many photosynthetic light harvesting complexes, formation of the S^* state does not lead to a loss of light harvesting efficiency by generating carotenoid triplet states on the ultrafast time scale, which may be related to the relaxed, planar, conformation of the triad-bound carotenoid in hexane solution. Upon completion of the light harvesting function, the carotenoids in triad **1** efficiently accept energy from phthalocyanine triplet states that have been formed through intersystem crossing, and do so at a rate that is much faster than the phthalocyanine singlet-state decay rate, $(5.6 \text{ ns})^{-1}$.

Our studies on triad **2**, which binds carotenoids with 10 conjugated carbon–carbon double bonds, have shown that accurate tuning of the energies of the optically forbidden states of the carotenoid relative to the states of the acceptor molecule are crucial for an efficient light harvesting function. We found that lowering of the S_1 state energy leads to a loss of overall energy transfer efficiency, which can be traced back to a decreased spectral overlap between donor and acceptor. The light-harvesting role of the S^* state could not unambiguously be elucidated for triad **2**, nor could the multiple quenching processes that govern the singlet state decay of the Pc. These will be the subject of further studies.

Finally, we have shown that the carotenoids serve as excellent electron donors to phthalocyanine in triads **1** and **2** when the molecules are dissolved in a polar solvent.

5. Appendix

To indicate the quality of the time-resolved spectra taken on triads **1** and **2** and illustrate their complex spectral evolutions in time, raw time-resolved spectra are shown in Figure 9, parts A (triad **2**) and B (triad **1**), at time delays indicated. Twelve out of a total of 120 spectra are shown for each triad. The SADS shown in Figure 4, parts A and B are derived from the complete datasets of 120 spectra.

Acknowledgment. This work was supported by the European Union – access to Research Infrastructures action of the Improving Human Potential Program (HPRI-CT-1999-00064), the U. S. Department of Energy (DE-FG02-03ER15393), the Earth and Life Sciences Council of The Netherlands Organization for Scientific Research (NWO-ALW), and The Netherlands Organization for Fundamental Research on Matter (FOM). We thank Roche for the generous gift of carotenoid samples. This is publication 579 from the ASU Center for the Study of Early Events in Photosynthesis.

References and Notes

- (1) Ritz, T.; Damjanovic, A.; Schulten, K.; Zhang, J.-P.; Koyama, Y. *Photosynth. Res.* **2000**, *66*, 125.
- (2) Koyama, Y.; Kuki, M.; Andersson, P. O.; Gillbro, T. *Photochem. Photobiol.* **1996**, *63*, 243.
- (3) Frank, H. A.; Cogdell, R. J. In *Carotenoids in Photosynthesis*; Young, A., Britton, G., Eds.; Chapman & Hall: London, 1993; p 252.
- (4) van Grondelle, R.; Dekker, J. P.; Gillbro, T.; Sundström, V. *Biochim. Biophys. Acta (Bioeng.)* **1994**, *1187*, 1.
- (5) Tracewell, C. A.; Vrettos, J. S.; Bautista, J. A.; Frank, H. A.; Brudvig, G. W. *Arch. Biochem. Biophys.* **2001**, *385*, 61.
- (6) Hanley, J.; Deligiannakis, Y.; Pascal, A.; Faller, P.; Rutherford, A. W. *Biochemistry* **1999**, *38*, 8189.
- (7) Horton, P.; Ruban, A. V.; Young, A. J. In *The Photochemistry of Carotenoids*; Frank, H. A., Britton, A. J. Y. G., Cogdell, R. J., Eds.; Kluwer Academic Publishers: Dordrecht, The Netherlands, 1999; p 271.
- (8) McDermott, G.; Prince, S. M.; Freer, A. A.; Hawthornthwaite-Lawless, A. M.; Papiz, M. Z.; Cogdell, R. J.; Isaacs, N. W. *Nature* **1995**, *374*, 517.
- (9) Jordan, P.; Fromme, P.; Witt, H. T.; Klukas, O.; Saenger, W.; Krauss, N. *Nature* **2001**, *411*, 909.
- (10) Kuhlbrandt, W.; Wang, D. N.; Fujiyoshi, Y. *Nature* **1994**, *367*, 614.
- (11) Koepke, J.; Hu, X. C.; Muenke, C.; Schulten, K.; Michel, H. *Structure* **1996**, *4*, 581.
- (12) Walla, P. J.; Linden, P. A.; Hsu, C. P.; Scholes, G. D.; Fleming, G. R. *Proc. Natl. Acad. Sci. (U.S.A.)* **2000**, *97*, 10808.
- (13) Zhang, J.-P.; Fujii, R.; Qian, P.; Inaba, T.; Mizoguchi, T.; Koyama, Y.; Onaka, K.; Watanabe, Y. *J. Phys. Chem. B* **2000**, *104*, 3683.
- (14) Gradinaru, C. C.; van Stokkum, I. H. M.; Pascal, A. A.; van Grondelle, R.; van Amerongen, H. *J. Phys. Chem. B* **2000**, *104*, 9330.
- (15) Shreve, A. P.; Trautman, J. K.; Frank, H. A.; Owens, T. G.; Albrecht, A. C. *Biochim. Biophys. Acta* **1991**, *1058*, 280.
- (16) Damjanovic, A.; Ritz, T.; Schulten, K. *Phys. Rev. E* **1999**, *59*, 3293.
- (17) Krueger, B. P.; Scholes, G. D.; Fleming, G. R. *J. Phys. Chem. B* **1998**, *102*, 5378.

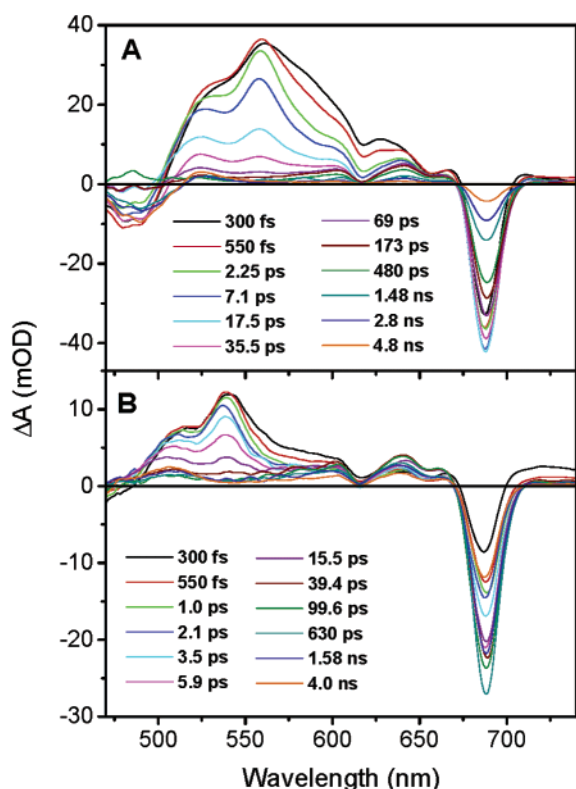


Figure 9. A: raw time-resolved spectra in triad **2** dissolved in *n*-hexane upon excitation at 475 nm, recorded at the time delays indicated. B: Same as A for triad **1**.

- (18) Gradinaru, C. C.; Kennis, J. T. M.; Papagiannakis, E.; van Stokkum, I. H. M.; Cogdell, R. J.; Fleming, G. R.; Niederman, R. A.; van Grondelle, R. *Proc. Natl. Acad. Sci. (U.S.A.)* **2001**, *98*, 2364.
- (19) de Weerd, F. L.; Dekker, J. P.; van Grondelle, R. *J. Phys. Chem. B* **2003**, *107*, 6214.
- (20) Croce, R.; Muller, M. G.; Bassi, R.; Holzwarth, A. R. *Biophys. J.* **2001**, *80*, 901.
- (21) Kennis, J. T. M.; Gobets, B.; van Stokkum, I. H. M.; Dekker, J. P.; van Grondelle, R.; Fleming, G. R. *J. Phys. Chem. B* **2001**, *105*, 4485.
- (22) de Weerd, F. L.; Kennis, J. T. M.; Dekker, J. P.; van Grondelle, R. *J. Phys. Chem. B* **2003**, *107*, 5995.
- (23) Papagiannakis, E.; Kennis, J. T. M.; van Stokkum, I. H. M.; Cogdell, R. J.; van Grondelle, R. *Proc. Natl. Acad. Sci. (U.S.A.)* **2002**, *99*, 6017.
- (24) Tavan, P.; Schulten, K. *J. Chem. Phys.* **1986**, *85*, 6602.
- (25) Sashima, T.; Nagae, H.; Kuki, M.; Koyama, Y. *Chem. Phys. Lett.* **1999**, *299*, 187.
- (26) Zhang, J.-P.; Inaba, T.; Watanabe, Y.; Koyama, Y. *Chem. Phys. Lett.* **2000**, *332*, 351.
- (27) Cerullo, G.; Polli, D.; Lanzani, G.; De Silvestri, S.; Hashimoto, H.; Cogdell, R. *J. Science* **2002**, *298*, 2395.
- (28) Tavan, P.; Schulten, K. *Phys. Rev. B* **1987**, *36*, 4337.
- (29) Marino-Ochoa, E.; Palacios, R.; Kodis, G.; Macpherson, A. N.; Gillbro, T.; Gust, D.; Moore, T. A.; Moore, A. L. *Photochem. Photobiol.* **2002**, *76*, 116.
- (30) Macpherson, A. N.; Liddell, P. A.; Kuciauskas, D.; Tatman, D.; Gillbro, T.; Gust, D.; Moore, T. A.; Moore, A. L. *J. Phys. Chem. B* **2002**, *106*, 9424.
- (31) Gust, D.; Moore, T. A.; Moore, A. L. *Acc. Chem. Res.* **2001**, *34*, 40.
- (32) Liddell, P. A.; Kuciauskas, D.; Sumida, J. P.; Nash, B.; Nguyen, D.; Moore, A. L.; Moore, T. A.; Gust, D. *J. Am. Chem. Soc.* **1997**, *119*, 1400.
- (33) Cardoso, S. L.; Nicodem, D. E.; Moore, T. A.; Moore, A. L.; Gust, D. *J. Am. Chem. Soc.* **1996**, *7*, 19.
- (34) Freiberg, A.; Timpmann, K.; Lin, S.; Woodbury, N. W. *J. Phys. Chem. B* **1998**, *102*, 10974.
- (35) van Stokkum, I. H. M.; Scherer, T.; Brouwer, A. M.; Verhoeven, J. W. *J. Phys. Chem. B* **1994**, *98*, 852.
- (36) Macpherson, A. N.; Gillbro, T. *J. Phys. Chem. A* **1998**, *102*, 5049.
- (37) Ricci, M.; Bradforth, S. E.; Jimenez, R.; Fleming, G. R. *Chem. Phys. Lett.* **1996**, *259*, 381.
- (38) Macpherson, A. N.; Arellano, J. B.; Fraser, N. J.; Cogdell, R. J.; Gillbro, T. *Biophys. J.* **2001**, *80*, 923.
- (39) Holt, N. E.; Kennis, J. T. M.; Dall'Osto, L.; Bassi, R.; Fleming, G. R. *Chem. Phys. Lett.* **2003**, *379*, 305.
- (40) Zhang, J.-P.; T., I.; Watanabe, Y.; Koyama, Y. *Chem. Phys. Lett.* **2000**, *331*, 154.
- (41) Polivka, T.; Herek, J. L.; Zigmantas, D.; Akerlund, H. E.; Sundstrom, V. *Proc. Natl. Acad. Sci. (U.S.A.)* **1999**, 4914.
- (42) Frank, H. A.; Cua, A.; Chynwat, V.; Young, A.; Gosztola, D.; Wasielewski, M. R. *Photosynth. Res.* **1994**, *41*, 389.
- (43) Desamero, R. Z. B.; Chynwat, V.; van der Hoef, I.; Jansen, F. J.; Lugtenburg, J.; Gosztola, D.; Wasielewski, M. R.; Cua, A.; Bocian, D. F.; Frank, H. A. *J. Phys. Chem. B* **1998**, *102*, 8151.
- (44) de Weerd, F. L.; van Stokkum, I. H. M.; van Grondelle, R. *Chem. Phys. Lett.* **2002**, *354*, 38.
- (45) Billsten, H. H.; Zigmantas, D.; Sundstrom, V.; Polivka, T. *Chem. Phys. Lett.* **2002**, *355*, 465.
- (46) Papagiannakis, E.; Das, S. K.; Gall, A.; van Stokkum, I. H. M.; Robert, B.; van Grondelle, R.; Frank, H. A.; Kennis, J. T. M. *J. Phys. Chem. B* **2003**, *107*, 5642.
- (47) Hsu, C. P.; Walla, P. J.; Head-Gordon, M.; Fleming, G. R. *J. Phys. Chem. B* **2001**, *105*, 11016.
- (48) Fujii, R.; Onaka, K.; Kuki, M.; Koyama, Y.; Watanabe, Y. *Chem. Phys. Lett.* **1998**, *288*, 847.
- (49) Frank, H. A.; Bautista, J. A.; Josue, J. S.; Young, A. J. *Biochemistry* **2000**, *39*, 2831.
- (50) Polivka, T.; Zigmantas, D.; Frank, H. A.; Bautista, J. A.; Herek, J. L.; Koyama, Y.; Fujii, R.; Sundstrom, V. *J. Phys. Chem. B* **2001**, *105*, 1072.
- (51) Polivka, T.; Zigmantas, D.; Herek, J. L.; He, Z.; Pascher, T.; Pullerits, T.; Cogdell, R. J.; Frank, H. A.; Sundstrom, V. *J. Phys. Chem. B* **2002**, *106*, 11016.
- (52) Andersson, P. O.; Gillbro, T. *J. Chem. Phys.* **1995**, *103*, 2509.
- (53) Yoshizawa, M.; Aoki, H.; Ue, M.; Hashimoto, H. *Phys. Rev. B* **2003**, *67*, 174302.
- (54) Yoshizawa, M.; Aoki, H.; Hashimoto, H. *Phys. Rev. B* **2001**, *63*, 180301.
- (55) McCamant, D. W.; Kim, J. E.; Mathies, R. A. *J. Phys. Chem. A* **2002**, *106*, 6030.
- (56) Rondonuwu, F. S.; Watanabe, Y.; Zhang, J. P.; Furuichi, K.; Koyama, Y. *Chem. Phys. Lett.* **2002**, *357*, 376.
- (57) McCamant, D. W.; Kukura, P.; Mathies, R. A. *J. Phys. Chem. A* **2003**, *107*, 8208.
- (58) Bittl, R.; Schlodder, E.; Geisenheimer, I.; Lubitz, W.; Cogdell, R. *J. J. Phys. Chem. B* **2001**, *105*, 5525.